

Solving the time-dependent Schrödinger equation using finite difference methods

R. Becerril^a, F.S. Guzmán^a, A. Rendón-Romero^b, and S. Valdez-Alvarado^a

^a Instituto de Física y Matemáticas, Universidad Michoacana de San Nicolás de Hidalgo. Edificio C-3,
Cd. Universitaria, 58040 Morelia, Michoacán, México.

^b Facultad de Ciencias Fisicomatemáticas, Universidad Michoacana de San Nicolás de Hidalgo. Edificio B,
Cd. Universitaria, 58040 Morelia, Michoacán, México.

Recibido el 9 de agosto de 2007; aceptado el 21 de febrero de 2008

We solve the time-dependent Schrödinger equation in one and two dimensions using the finite difference approximation. The evolution is carried out using the method of lines. The illustrative cases include: the particle in a box and the harmonic oscillator in one and two dimensions. As non-standard examples we evolve two solitons and show the time-dependent solitonic behavior in one dimension and the stabilization of an atomic gas model in two dimensions. The codes used to generate the results in this manuscript are freely available under request, and we expect this material could help students to have a better grasp of the solution of partial differential equations related to dynamical systems.

Keywords: Finite difference methods; computational techniques; Schrödinger equation.

Resolvemos la ecuación de Schrödinger dependiente del tiempo en una y dos dimensiones usando diferencias finitas. La evolución se lleva a cabo usando el método de líneas. Los casos ilustrativos incluyen: la partícula en una caja y en un potencial de oscilador armónico en una y dos dimensiones. Como ejemplos poco comunes presentamos la evolución de dos solitones y mostramos la dependencia temporal del comportamiento solitónico en una dimensión y la estabilización de un modelo de gas atómico en dos dimensiones. Los códigos usados para generar los resultados en este manuscrito se encuentran disponibles a la menor petición, y esperamos que este hecho ayude a los estudiantes a adquirir un mejor entendimiento de la solución de ecuaciones diferenciales parciales relacionadas con sistemas dinámicos.

Descriptores: Método de diferencias finitas; técnicas computacionales; ecuación de Schrödinger.

PACS: 02.70.Bf; 02.70.-c

1. Introduction

Numerical methods have been very important in basic research on physics. Nowadays partial differential equations (PDEs) related to main stream problems involve the use of numerical solutions to PDEs. As examples we mention a few:

- 1) numerical relativity, related to the set of highly non-linear systems of coupled differential equations of general relativity, which have to be solved under very general symmetry conditions in order to predict the profile of gravitational waves that are expected to be observed by ground-based gravitational wave detectors;
- 2) Euler's equations, where the numerical solution to PDEs is essential, because the hydro-dynamical equations must be solved either for comparison between theory and laboratory experiments or on an astrophysical scale, where these equations must be solved in order to explain and predict astrophysical phenomena, such as the physical conditions of the supernovae core-collapse;
- 3) a problem more related to the system we deal with in this paper, the evolution of a Bose condensate in the mean field approximation, which involves the solution of the time-dependent Schrödinger equation with potentials including corrections of self-interaction between pairs of particles, the so-called Gross-Pitaevskii equation [1].

Thus, numerical solutions to PDEs should be made available to any student, as a tool for tackling problems with approximate methods that could help explain experimental results or provide predictions of theoretical branches of physics.

This is expected to be the first of a series of papers in which we illustrate the solution of PDEs and provide the code. In this first manuscript we present the numerical solution to Schrödinger's equation in various situations: one and two dimensions for classical problems whose solutions are known, employing the finite difference (FD) method, and using the method of lines to integrate in time. The basic idea of the FD approach is to replace function derivatives by differences in that function evaluated at certain neighboring points in the domain, so that the solution is given solely for that set of points. Spectral methods will be used in subsequent papers to solve hyperbolic equations in one and two dimensions, and other important equations in physics, particularly in fluid dynamics.

The main goal of these papers is to introduce students to a very basic approach to the numerical solution of some equations in physics. We expect that the fact of presenting a fully working code that students can modify stimulates the use of numerical methods to solve problems related to particular research topics.

This first paper involves what we consider the simplest case: the 1D and 2D Schrödinger equation for a particle in a box and a particle in a harmonic oscillator potential; we also

evolve two solitons in one spatial dimension and the stabilization of an atomic gas in two dimensions.

The code we use to compute the results in this paper is available on request, and this paper would serve to document it. This type of code is expected to be a starting point for students in Physics who want to solve PDEs related to different problems; the code used in the solution of the present problems could be used - possibly with minor modifications- to solve several other time-dependent problems.

As an extra bonus, we rewrite the exact solutions to the classical problems in quantum mechanics in full space and time dependence. We do so, because we consider that coding the solution to partial differential equations involves an adequate knowledge of exact solutions to well known cases.

This paper is organized as follows: in Sec. 2 we present the finite differences approximation of partial differential equations in one dimension; in Sec. 3 we solve Schrödinger's equation in one dimension; in Sec. 4 we develop the finite differences approximation in 2 dimensions; and in Sec. 5 we solve Schrödinger's equation in 2D. Finally, in Sec. 6 we draw some final conclusions.

2. Approximation using finite differences in 1D

2.1. Taylor expansions

There are different approximations of the system of equations to be solved: for example, spectral methods assume that the functions involved in the system of differential equations can be expanded as a series of orthogonal functions on a given domain; then orthogonality conditions and recurrence relations are used to reduce the system to a simpler system of equations for the coefficients of the expansion. This is a case studied in depth in a forthcoming paper [2].

The approximation using finite differences works in a different way. In order to illustrate how discretization works in an Initial Value Problem, we assume the case of a hypothetical finite domain with a time coordinate t and a spatial coordinate x . Spatial coordinates are defined as a discrete set of points given by $x_j = j\Delta x$, and the boundaries correspond to the points x_0 (on the left) and x_N (on the right). Time $t^n = n\Delta t$ is also defined only for certain values of the continuum time. Thus, a function is defined only for the values of x and t that correspond to points in the mesh in such a way that for a given continuous function f there are available values of it at (t^n, x_j) , denoted here by f_j^n . For a uniformly discretized domain, $\Delta x = x_{i+1} - x_i$ and $\Delta t = t^{n+1} - t^n$, indicate the resolution in the spatial and time coordinates respectively. Once we have defined an approximate discrete domain, we proceed to define an approximation of a PDE.

The finite difference approximation assumes that the functions involved can be expanded in a Taylor series around every point of the mesh up to a desired order of approximation. Therefore, considering the function f is defined and smooth at every x_i , the value of the function for the nearest

neighbors can be calculated as follows:

$$\begin{aligned} f(x_{j-1}) &= f(x_j) - \Delta x f'(x_j) + \frac{\Delta x^2}{2} f''(x_j) \\ &\quad - \frac{\Delta x^3}{6} f'''(x_j) + O(\Delta x^4), \\ f(x_j) &= f(x_j), \\ f(x_{j+1}) &= f(x_j) + \Delta x f'(x_j) + \frac{\Delta x^2}{2} f''(x_j) \\ &\quad + \frac{\Delta x^3}{6} f'''(x_j) + O(\Delta x^4), \end{aligned}$$

where the prime denotes the derivative with respect to x . Starting from these approximations it is possible to construct difference operators for the derivatives of f_i^n . For instance, by adding the first and third expressions one obtains an expression for the first derivative at the point x_j with a second-order error

$$f'(x_j) = \frac{f(x_{j+1}) - f(x_{j-1})}{2\Delta x} + O(\Delta x^2);$$

notice that the value of the function for the left and right nearest neighbors is needed in order to calculate this derivative, which is why this combination is called a centered finite difference approximation.

In order to obtain the second derivative of f , it suffices to write the combination

$$\frac{f(x_{j+1}) - 2f(x_j) + f(x_{j-1})}{\Delta x^2} = f''(x_j) + O(\Delta x^2),$$

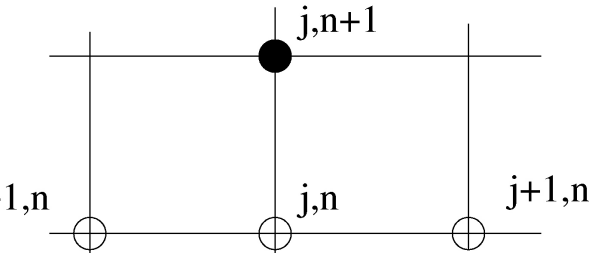


FIGURE 1. Illustration of the molecule used to construct f at the $n+1$ time slice. A filled circle indicates the place where one wishes to find the desired variable onto, and empty circles indicate the location where the functions involved are known.

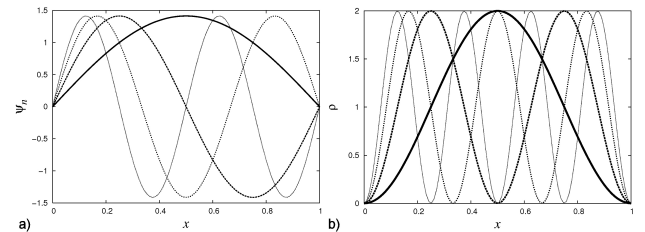


FIGURE 2. Exact solution for the particle in a one-dimensional box. (Left) Real part of the wave function Ψ for the particle in a box with $n_x = 0, 1, 2, 3, 4$ at $t = 0$. (Right) Density of probability for the same cases.

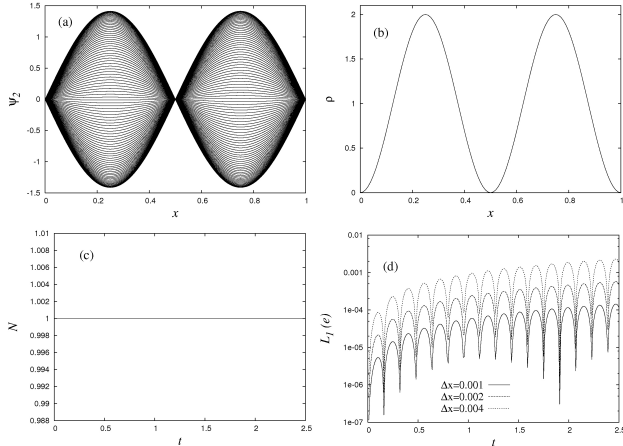


FIGURE 3. Numerical solution for the particle in a one-dimensional box. (a) Real part of the wave function Ψ for a particle in a box, with $n_x = 2$ for several times. (b) Density of probability also for several values of time. The time-independence of ρ is manifest. The resolution used is $\Delta x = 0.001$. (c) The integral $N = \int_0^1 \rho dx$ which remains constant in time. (d) The L_1 norm of e , defined as $L_1(e) = \sum_i |e_i|$ for every x_i . This quantity for $\Delta x = 0.004$ is four times that for $\Delta x = 0.002$, which in turn is four times that found for $\Delta x = 0.001$.

which implies the desired expression for the second derivative with second-order accuracy as well. As in the previous case, this is also a centered approximation of the second derivative.

In the location of the spatial boundaries, one of the nearest neighbors would be missing (for the point x_0 the left point x_{-1} is not defined), and a centered approximation would require the addition of an extra point (a ghost point) to the domain; in most problems it is preferable to live without ghost points for the purpose of imposing boundary conditions. Therefore we consider that only points to the right in the spatial domain are available (in the case of the left boundary), thus we proceed by writing the approximations of the function considering only points on the right as follows:

$$\begin{aligned} f(x_j) &= f(x_j), \\ f(x_{j+1}) &= f(x_j) + \Delta x f' + \frac{\Delta x^2}{2} f'' + O(\Delta x^3), \\ f(x_{j+2}) &= f(x_j) + 2\Delta x f' + 2\Delta x^2 f'' + O(\Delta x^3). \end{aligned} \quad (1)$$

The combination

$$f(x_{j+2}) - 4f(x_{j+1}) + 3f(x_j) = 2\Delta x f' + O(\Delta x^3)$$

implies the desired expression for the first spatial derivative of the function with second-order accuracy; when applied to the left boundary it would read

$$f'_0 = \frac{f(x_2) - 4f(x_1) + 3f(x_0)}{2\Delta x} + O(\Delta x^2).$$

A similar expression can be obtained for the right boundary considering only points to the left.

Approximation of derivatives with respect to time can be obtained in the same way as the spatial derivatives, one only needs to vary the time labels (n) instead of the space labels (j). For a complete description of the discrete version of operators see [3].

2.2. The evolution

The evolution of data consists in calculating the function f_j^{n+1} from data in the previous time slices f_j^n , f_j^{n-1} , f_j^{n-2} etc. In order to illustrate this fact, consider the diffusion equation $\partial f / \partial t = \partial^2 f / \partial x^2$. The discretized version of this equation centered at (t^n, x_j) is:

$$\frac{f_j^{n+1} - f_j^{n-1}}{2\Delta t} = \frac{f_{j+1}^n - 2f_j^n + f_{j-1}^n}{\Delta x^2} + O(\Delta x^2, \Delta t^2), \quad (2)$$

where the results of finite differencing above have been used assuming Δt and Δx to be small. In (2) it is possible to solve for f_j^{n+1} , that is, the value of f at time t^{n+1} can be found in terms of its values at previous time levels. When this is possible the method is called explicit. Notice that in order to calculate the values of f^{n+1} , values of f^n and f^{n-1} are required, that is, three time levels are needed; this is an example of an explicit method (as done in Ref. 4). In practice, one defines arrays for each variable (say f) for the number of time levels needed (3 with this discretization), and as long as one is working in one dimension there are no problems of allocatable memory, however, when one deals with equations in two and three dimensions, the memory becomes an important problem. That is why we introduce once for all the notion of the Method of Lines (MoL), which only requires two time levels. In the method of lines approach, the FD approximation is written in a semi-discrete form as

$$\frac{\partial f}{\partial t} = \frac{f_{j+1}^n - 2f_j^n + f_{j-1}^n}{\Delta x^2} + O(\Delta x^2). \quad (3)$$

The molecule associated with this discretization can be found in Fig. 1 for each j . Then, it is assumed that for each j , f , satisfies an ordinary differential equation (ODE) along the vertical lines of the domain (see Fig. 1). With this in mind, it suffices to have the discretization in (3) and integrate the resulting differential equation in time for $\partial f / \partial t$. Terms other than the time derivative of f are considered to belong to the right-hand side of the ODE in time. Thus only an ODE integrator is required to evolve the data from one time slice to the next. One only needs to choose the integrator, which is selected according to the accuracy, dissipation and stability properties that depend on the restrictions on the factor $\Delta t / \Delta x^2$ (to learn about the properties of evolution algorithms we refer the reader to Refs. 3, 5 to 7). In the present paper, the third-order Runge-Kutta algorithm is the one used for the evolution. A simplified but practical illustration of this algorithm assumes the unknown function f to be such that $\partial_t f = S$, where S would be, for instance, the right-hand side (RHS) in (3). A naive way to solve this equation would be to replace it by $f^{n+1} = f^n + \Delta t S^n$, a procedure known as the Euler method,

which is neither accurate nor stable. The Euler method can be thought of as a first-order Runge Kutta Method, which evaluates derivatives (S^n) only at the time slice (t^n), which makes this method very asymmetric with respect to the beginning and end of intervals. To remedy this, one makes an Euler-like trial step to the midpoint to compute the real step across the whole interval Δt , having in this manner a single-step method, but double-stage time discretization. Namely,

$$\begin{aligned} k_1 &= \Delta t S(t^n, f^n), \\ k_2 &= \Delta t S(t^n + \Delta t/2, f^n + k_1/2), \\ f^{n+1} &= f^n + k_2 + O(\Delta t^3) \\ &= f^n + \Delta t S(t^n + \Delta t/2, f^n + k_1/2) + O(\Delta t^3). \end{aligned} \quad (4)$$

Symmetrization cancels out the first-order error term, yielding a second-order accuracy method (Runge Kutta 2). By using two trial steps per time interval, it is possible to cancel out first- and second-order error terms and construct a third-order Runge Kutta method. The second trial step would be given by $k_3 = \Delta t S(t_n + \Delta t/2, f^n + k_2/2)$, and then the algorithm for calculating f^{n+1} in terms of the values of f^n would read:

$$\begin{aligned} k_1 &= \Delta t S(t^n, f^n), \\ k_2 &= \Delta t S(t^n + \Delta t/2, f^n + k_1/2), \\ k_3 &= \Delta t S(t^n + \Delta t/2, f^n + k_2/2), \\ f^{n+1} &= f^n + \frac{1}{6}k_1 + \frac{2}{3}k_2 + \frac{1}{6}k_3. \end{aligned} \quad (5)$$

This algorithm is widely used because it requires only three iterations and is accurate and stable for small enough values of the $\Delta t/\Delta x^2$ factor.

In a few words, the way we solve the time-dependent Schrödinger equation will be based on the *evolution of the initial data*. That is, given a wave function at initial time t^0 , the values of the wave function at subsequent time slices are calculated using the evolution under a MoL discretization. In the case of the particle in a box and the harmonic oscillator we shall use the exact solution at the initial time as the initial data for the wave function. In the case of solitons we shall also use two superposed exact solitons as initial data and in the atomic gas model we start with a Gaussian initial wave function.

3. 1D Schrödinger Equation

The general form of the one-dimensional Schrödinger equation is

$$i\hbar \frac{\partial \Psi(x, t)}{\partial t} = -\frac{\hbar^2}{2m} \frac{\partial^2 \Psi(x, t)}{\partial x^2} + V(x, t)\Psi(x, t). \quad (6)$$

It is important, when calculating numerical solutions, to get rid of constants that are either tiny or huge. That is why atomic units are used, that is $\hbar = m = 1$. We shall assume these units in the rest of the paper. Next we present particular solutions to this equation.

3.1. Particle in a 1D box

3.1.1. Exact solution

In this case we choose the domain to be $x \in [0, 1]$. The particle is considered to be free in the domain, that is $V = 0$, except at the boundaries, where V is assumed to be infinite in order to model the effects of a solid wall of a box; thus the boundary conditions are $\Psi(x = 0, t) = \Psi(x = 1, t) = 0$. If one separates variables, the wave function can be expressed as $\Psi(x, t) = \psi(x)e^{-iEt}$, and the remaining equation for $\psi(x)$ reads:

$$\frac{\partial^2 \psi}{\partial x^2} + 2E\psi = 0. \quad (7)$$

Applying the conditions of continuity of ψ and its derivative at the boundaries, we know the solution is:

$$\psi_{n_x}(x) = A_{n_x} \sin(n_x \pi x), \quad E_{n_x} = \frac{(n_x \pi)^2}{2}.$$

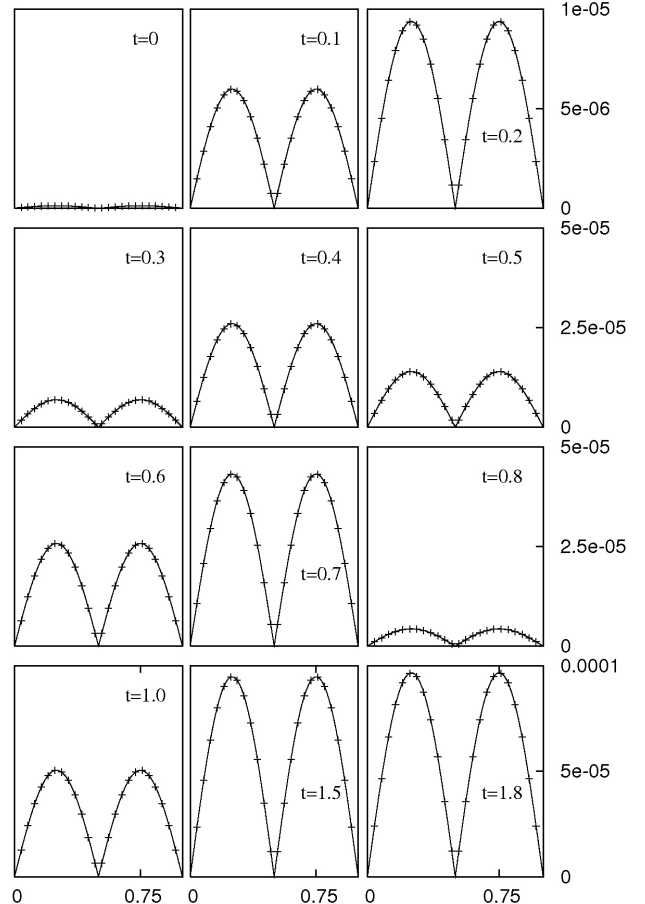


FIGURE 4. Snapshots of the error for two different resolutions for the evolution shown in the previous figure. The numerical solution shows second-order convergence. The resolutions used are $\Delta x = 0.001$ and $\Delta x = 0.002$. The continuous lines represent the error calculated with $\Delta x = 0.001$, and the dots indicate the error calculated using $\Delta x = 0.002$ divided by 4 (only at a few points, so that it is possible to appreciate the plot).

where $n_x = 0, 1, 2, \dots$ is the quantum number labeling the permitted energy values. After demanding the normalization of the wave function

$$\int_0^1 \psi^* \psi dx = \int_0^1 A_{n_x}^2 \sin^2(n_x \pi x) dx = 1,$$

we find that $A_{n_x}^2 / 2 = 1$, that is: $A_{n_x} = \sqrt{2}$, which finally implies $\psi_{n_x}(x) = \sqrt{2} \sin(n_x \pi x)$. Therefore, the complete time-dependent solution is:

$$\Psi_{n_x}(x) = \sqrt{2} e^{-i E_{n_x} t} \sin(n_x \pi x). \quad (8)$$

In order to compare the numerical solution with the exact solution, we shall only use the real part of it:

$$\Re(\Psi_{n_x}(x, t)) = \sqrt{2} \cos(E_{n_x} t) \sin(n_x \pi x). \quad (9)$$

The energy density calculated from (8) is $\rho = \Psi^* \Psi = 2 \sin^2(n_x \pi x)$, which is evidently time independent. The time-independence serves to test any numerical solution, which must show a harmonic time-dependence of Ψ whereas ρ must remain constant in time.

An important lesson in working out a numerical solution, is that one actually has to develop all the constants involved, and keep in mind the domain, because a general solution needs all the parameters and constants of integration to be fixed. In Fig. 2 we show the exact solution at $t = 0$ for various values of n_x .

3.1.2. Numerical solution

The discretized version of (6) for the present case ($V = 0$) is as follows:

$$\frac{\partial \Psi}{\partial t} = \frac{i}{2} \frac{\Psi_{j+1}^n - 2\Psi_j^n + \Psi_{j-1}^n}{\Delta x^2} + O(\Delta x^2). \quad (10)$$

The right-hand side of this equation plays the role of S in (5). In order to test whether a numerical implementation is correct, one must reproduce the full time-dependent exact solution and show that the density of probability is actually time-independent. Moreover, we define an error on the real part of the wave function by

$$e = \Re(\Psi_{num}) - \Re(\Psi_{ex}), \quad (11)$$

where Ψ_{num} and Ψ_{ex} are the numerical and exact solutions respectively. In Fig. 3 we show the evolution of the initial wave function $\Psi_2(x, 0) = \sqrt{2} \sin(2\pi x)$, which is the solution of a particle in a box with 2 nodes. The density of probability is also shown and is manifestly time-independent. An important quantity is the integral

$$N = \int_0^1 \rho dx,$$

which determines whether or not an evolution algorithm is actually unitary or not; we show here that the method of lines

is able to keep this number constant. Finally also the convergence of the L_1 norm of the error to zero is shown. This last plot in Fig. 3 is quite important when showing numerical solutions of PDEs, and one cannot trust the numerical results obtained, unless there is an indication that the error of a solution converges to zero in the continuum limit (that is, when $\Delta x, \Delta t \rightarrow 0$).

Aside from the result showing the convergence of $L_1(e)$, one should verify, at least for a few snapshots, that the error is actually converging to zero, not only a norm of it, but the error itself. In Fig. 4 we show the error for two different resolutions. The fact that when doubling the resolution the error is four times smaller indicates second-order convergence of the solution (see Ref. 8 for details about convergence). What can be seen also in this plot, is that the error is growing in time. One important criterion to trust in numerical results is that one must be able to monitor the numerical error and determine the admitted tolerance for a solution, that is, one is able to decide from what values of the error on, one cannot trust the numerical results anymore.

3.2. Harmonic oscillator

3.2.1. Exact solution

In this case the potential is

$$V(x) = \frac{1}{2} kx^2.$$

Once again the solution using separation of variables can be written as $\Psi(x, t) = \psi(x)e^{-iEt}$ and the resulting Schrödinger equation is

$$\frac{d^2\psi}{dx^2} + [\beta - \alpha^2 x^2]\psi = 0, \quad (12)$$

where $\alpha = \sqrt{k}$ and $\beta = 2E$. Defining the new variable $\xi = \sqrt{\alpha}x$, one obtains

$$\frac{d^2\psi}{d\xi^2} + \left(\frac{\beta}{\alpha} - \xi^2\right)\psi = 0. \quad (13)$$

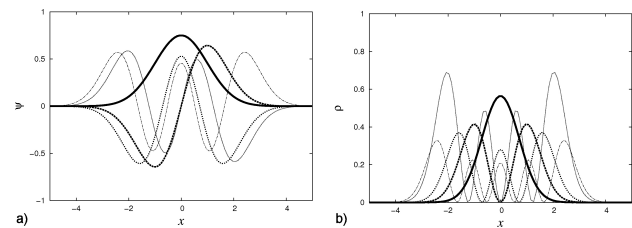


FIGURE 5. Exact solution of the one-dimensional harmonic oscillator. (Left) Real part of the wave function Ψ for $n_x = 0, 1, 2, 3, 4$. (Right) Density of probability for the same cases.

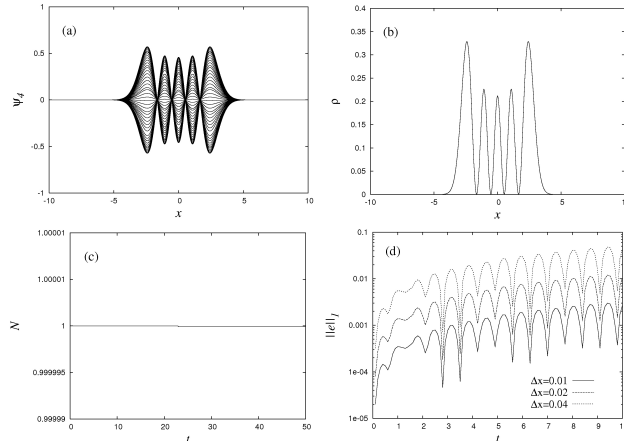


FIGURE 6. Numerical solution of the one-dimensional harmonic oscillator. (a) Real part of Ψ_{n_x} calculated for the harmonic oscillator and $n_x = 4$ for several times is shown. (b) Density of probability also for several times. The time-independence of ρ is manifest. The resolution used is $\Delta x = 0.01$. (c) The integral $N = \int \rho dx$ remains constant in time. (d) The L_1 norm of e . This quantity for $\Delta x = 0.04$ is four times that for $\Delta x = 0.02$, which in turn is four times that found for $\Delta x = 0.01$. This indicates that the error converges with second order to zero [8].

We look for bounded solutions for $\xi \rightarrow \pm\infty$, and we know such solutions satisfy

$$\psi(\xi) = e^{-\xi^2/2} H(\xi),$$

where now the equation for the H is Hermite's equation

$$\frac{d^2H}{d\xi^2} - 2\frac{dH}{d\xi} + \left(\frac{\beta}{\alpha} - 1\right) H = 0, \quad (14)$$

whose solutions are the Hermite polynomials

$$\begin{aligned} H_0(\xi) &= 1, \\ H_1(\xi) &= 2\xi, \\ H_2(\xi) &= 2 - 4\xi^2, \\ H_3(\xi) &= 12\xi - 8\xi^3, \\ H_4(\xi) &= 12 - 48\xi^2 + 16\xi^4, \end{aligned} \quad (15)$$

and so on. Thus the normalized solution for $\psi(x)$ is obtained from

$$\begin{aligned} \int_{-\infty}^{\infty} \psi^* \psi dx &= 1 : \\ \psi_{n_x}(\xi) &= \sqrt{\frac{1}{\sqrt{\pi} 2^{n_x} n_x!}} e^{-\xi^2/2} H_{n_x}(\xi), \end{aligned}$$

with $n_x = 0, 1, 2, \dots$. Recovering the original variables and the time dependence of Ψ , one finds

$$\Psi_{n_x}(x, t) = \sqrt{\frac{1}{\sqrt{\pi} 2^{n_x} n_x!}} e^{-iE_{n_x}t} e^{-x^2/2} H_{n_x}(x). \quad (16)$$

Once again we use the real part of this solution in order to measure the accuracy of the numerical solution:

$$\Re(\Psi_{n_x}(x, t)) = \sqrt{\frac{1}{\sqrt{\pi} 2^{n_x} n_x!}} e^{-x^2/2} H_{n_x}(x) \cos\left(\left(n_x + \frac{1}{2}\right)t\right). \quad (17)$$

We show this exact solution at $t = 0$ for various values of n_x and also the density of probability in Fig. 5.

3.2.2. Numerical solution

The method of lines discretization for the Schrödinger equation in this case is

$$\frac{\partial \Psi}{\partial t} = \frac{i}{2} \frac{\Psi_{j+1}^n - 2\Psi_j^n + \Psi_{j-1}^n}{\Delta x^2} - \frac{i}{2} x_j^n + O(\Delta x^2). \quad (18)$$

The boundary conditions are a subtle point. When constructing the exact solution, the wave function is required to vanish at infinity, so that the integral of the density of probability is

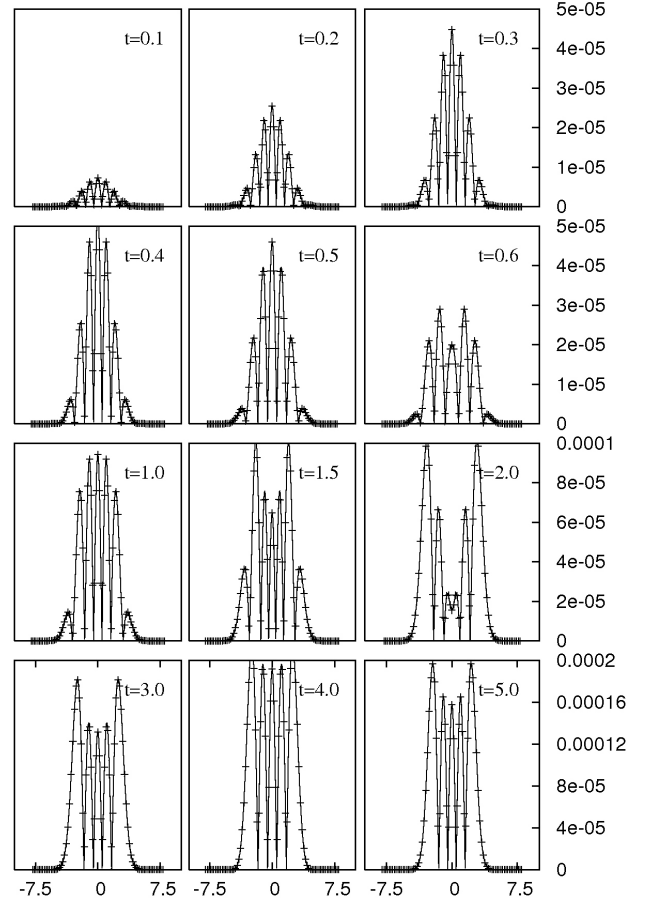


FIGURE 7. Snapshots of the error using two different resolutions $\Delta x = 0.01, 0.02$ for the evolution presented in the previous figure. The continuous lines represent the error calculated with $\Delta x = 0.01$, and the dots indicate the error calculated using $\Delta x = 0.02$ divided by 4 (only at a few points, so that it is possible to appreciate the plot). The fact that when doubling the resolution the error is four times smaller indicates second-order convergence to zero.

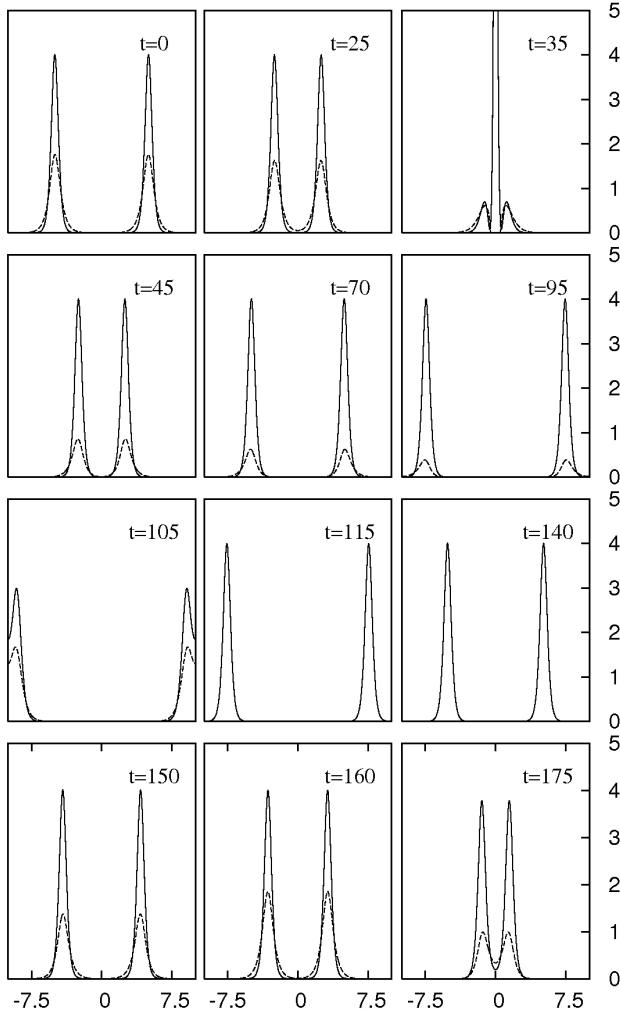


FIGURE 8. Evolution of two solitonic solutions on the same spatial domain with periodic boundary conditions. The expected behavior is manifest: the density profile -indicated with the solid line- of each of the initial superposed solutions maintain its shape even after the two blobs interact with each other. The dotted line indicates the real part of the wave function. At $t \sim 35$ the two blobs are shown to interact and form a sort of momentary interference pattern.

finite. What we have done here is to use a large enough domain so that the wave function is smaller than 10^{-15} , so that one needs to apply the same boundary as for the particle in a box, that is, the wave function is zero at the boundary. The evidence that the algorithm and boundary conditions together work well is shown in Fig. 6, where we present $\Re(\Psi)$ and ρ calculated numerically for $n_x = 4$. The wave function is oscillating (preserving the location of the nodes), whereas the density of probability remains time-independent.

In Fig. 7 we show the error for two different resolutions. Again, the fact that when doubling the resolution the error is four times smaller indicates second order convergence of the solution.

3.3. Solitons in one dimension

A slightly different problem is that of the solitonic behavior. Solitons are standing wave solutions to the non-linear Schrödinger equation for which the density profile of the solution is preserved during the evolution. In order to show that our algorithm works also in the non-linear case, here we show the evolution of the solution

$$\psi = a \frac{\exp[i(vx + (a^2 - v^2)t/2 - t_0)]}{\cosh[a(x - vt - x_0)]} \quad (19)$$

which is a standing wave function with amplitude a , speed v and initial time and position t_0 and x_0 , respectively. This is a solution to the non-linear Schrödinger equation:

$$i\partial_t \psi = -\frac{1}{2} \frac{\partial^2 \psi}{\partial x^2} - |\psi|^2 \psi \quad (20)$$

and is called a solitonic solution [9]. An important property of this type of solution is that it shows a density of probability that preserves its profile in time (even if it moves across the spatial domain) as a result of the balance between the focusing tendency of the wave function and the dispersive effect of the non-linear term. These solutions also propagate at a constant speed. Especially important is the case in which more than one of these solutions are evolved over the same spatial domain. In fact solitons in a more precise language are not only standing waves travelling at a constant speed with a constant density profile, but these solutions have the property of maintaining the shape of the density profile even when there is interaction with other solitons [10]. In Figs. 8 and 9 we show snapshots of two solutions like those of the type (19) superposed with parameters $a = 2$, $v = \pm 0.1$, $t_0 = 0$ and $x_0 = \pm 5$. The system is evolved using periodic boundary conditions, so that it is possible to track the evolution of the system for various crossing times and see the solitonic behavior several times.

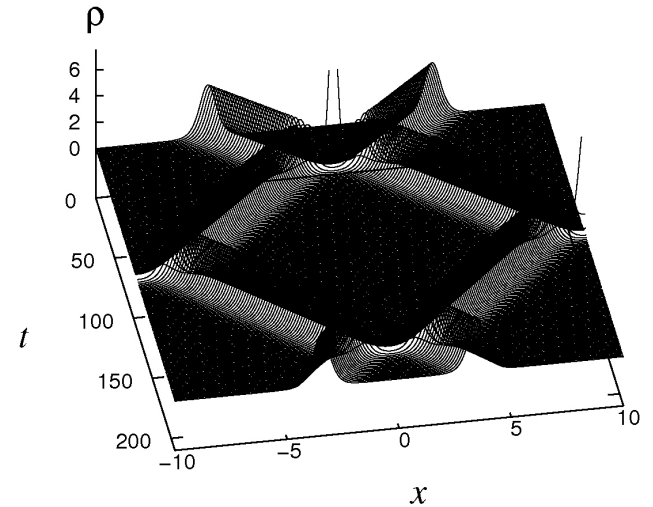


FIGURE 9. Density profile in time for the two solitons, where periodic boundary conditions are used. This simulation was carried out with a value $\Delta t/\Delta x^2 = 0.01$ and resolution $\Delta x = \Delta y = 0.025$.

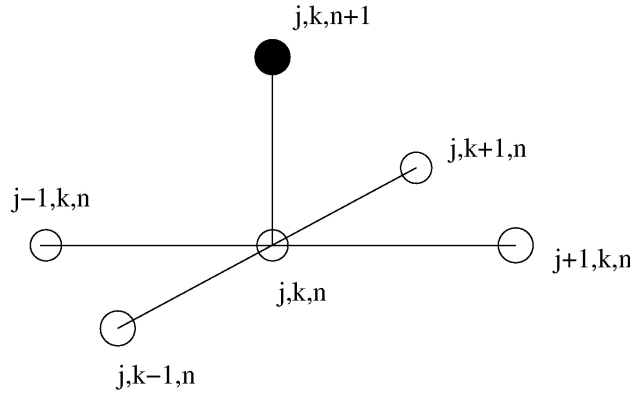


FIGURE 10. Illustration of the molecule used to construct f at the $n + 1$ time slice. A filled circle indicates the place where one wishes to find the desired variable onto, and empty circles indicate the location where the functions involved are known.

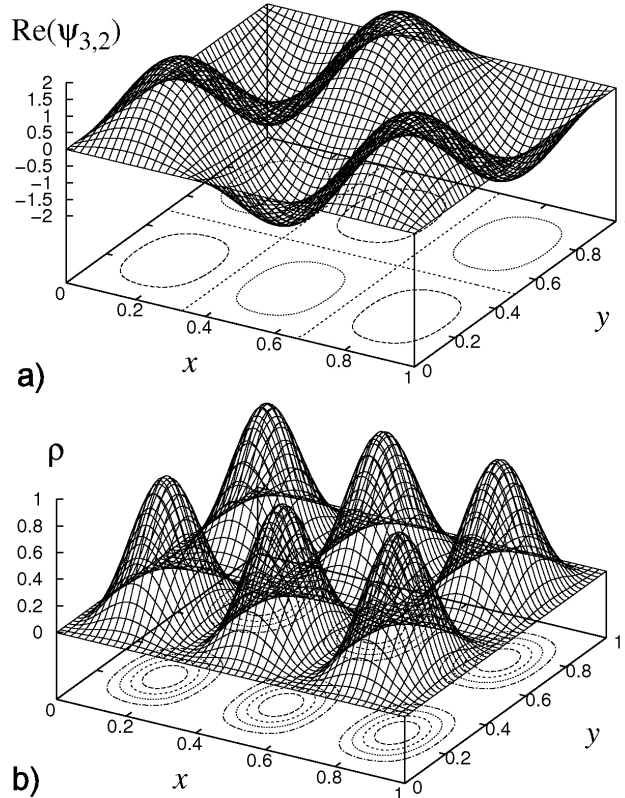


FIGURE 11. Exact solution for the particle in a two-dimensional box. We show the real part of the wave function (top) and the density of probability (bottom) for the case $n_x = 3$ and $n_y = 2$.

4. Approximation using finite differences in 2D

The FD approximation in two dimensions is an extension of that in one dimension. Assuming a function g depending on two spatial dimensions and time, a two-dimensional mesh is defined so that $x_j = j\Delta x$, $y_k = k\Delta y$, and again $t^n = n\Delta t$. Then the function is defined only at points $g_{j,k}^n = g(t^n, x_j, y_k)$. Its time derivatives are obtained in

the same way as before, and the spatial derivatives are constructed only by varying the index that labels the corresponding coordinate, that is:

$$\begin{aligned}\frac{\partial g(x_j, y_k)}{\partial x} &= \frac{g_{j+1,k} - g_{j-1,k}}{2\Delta x} + O(\Delta x^2) \\ \frac{\partial g(x_j, y_k)}{\partial y} &= \frac{g_{j,k+1} - g_{j,k-1}}{2\Delta y} + O(\Delta y^2)\end{aligned}\quad (21)$$

for all t^n , and analogous expressions for second derivatives. The concept of the method of lines is exactly the same as in the one-dimensional case. Then when the method of lines discretization is to be applied, the molecule considered to evolve a function from t^n to t^{n+1} is illustrated in Fig. 10.

5. 2D Schrödinger Equation

In two dimensions and Cartesian coordinates (x, y) , and using units where $\hbar = m = 1$ as before, the Schrödinger equation reads:

$$i \frac{\partial \Psi(x, y, t)}{\partial t} = -\frac{1}{2} \left(\frac{\partial^2 \Psi(x, y, t)}{\partial x^2} + \frac{\partial^2 \Psi(x, y, t)}{\partial y^2} \right) + V(x, y, t) \Psi(x, y, t).$$

The exact solution for the particle in a box and the harmonic oscillator is found through $\Psi(x, y, t) = \psi(x, y)e^{-iEt}$. The discrete approximation in two dimensions is an extension of the one-dimensional molecule as shown in Fig. 10.

5.1. Particle in a 2D box

5.1.1. Exact solution

In this case we choose the domain to be $\mathcal{D} = [0, 1] \times [0, 1]$. After the separation of variables mentioned above, the remaining equation to be solved in x and y is

$$\left(\frac{\partial^2 \psi}{\partial x^2} + \frac{\partial^2 \psi}{\partial y^2} \right) + 2E\psi = 0,$$

which again permits a separation of variables of the type $\psi(x, y) = X(x)Y(y)$. The boundary conditions again are $\Psi = 0$ on all faces of the boundary of \mathcal{D} . After applying these conditions and the normalization condition

$$\int_0^1 \int_0^1 \psi^* \psi dx dy = 1,$$

the exact solution reads:

$$\begin{aligned}\psi_{n_x, n_y} &= 2 \sin(n_x \pi x) \sin(n_y \pi y), \\ E_{n_x, n_y} &= \frac{\pi^2}{2} [(n_x^2) + (n_y^2)],\end{aligned}$$

where n_x and n_y are the quantum numbers that label an energy state and indicate the number of nodes along x and y . The complete time-dependent solution is then

$$\Psi = 2e^{-iE_n t} \sin(n_x \pi x) \sin(n_y \pi y),$$

from which we take its real part in order to compare with numerical results:

$$\Re(\Psi) = 2 \cos(E_n t) \sin(n_x \pi x) \sin(n_y \pi y).$$

As an example, we show in Fig. 11 the exact solution with $n_x = 3$ and $n_y = 2$ at $t = 0$. Our code should be able to show the oscillating wave function and a time-independent density of probability.

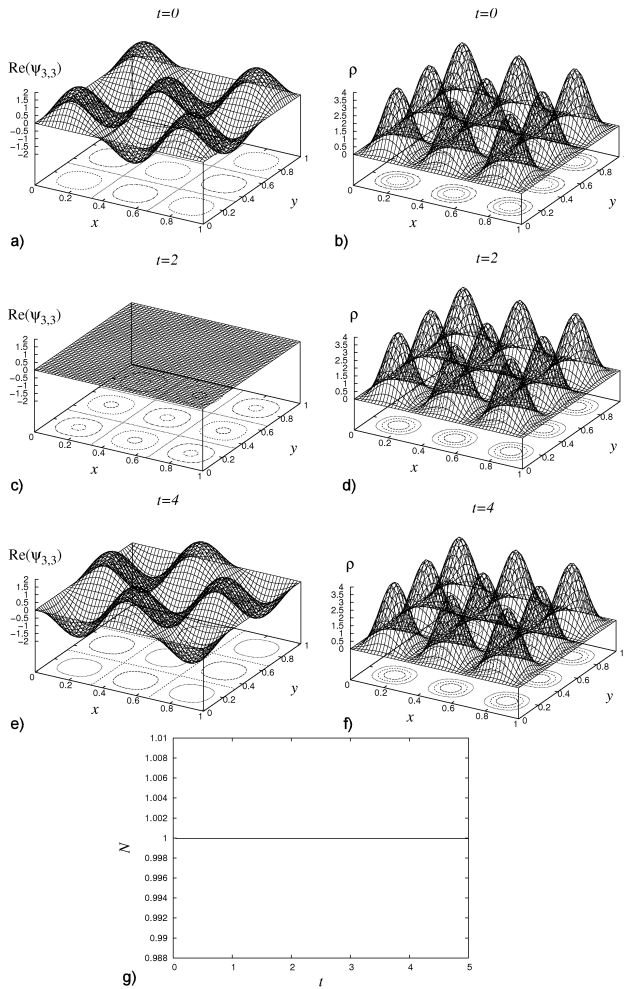


FIGURE 12. Numerical solution for the particle in a two dimensional box. We show the wave function and the density of probability for the case $n_x = 3$ and $n_y = 3$ at times $t = 0, 2, 4$. These plots were obtained using the resolution $\Delta x = \Delta y = 0.01$ and the factor $\Delta t/\Delta x^2 = 0.1$. The wave function is oscillating, the density of probability ρ is constant in time, and so its integral $N = \int pdxdy$.

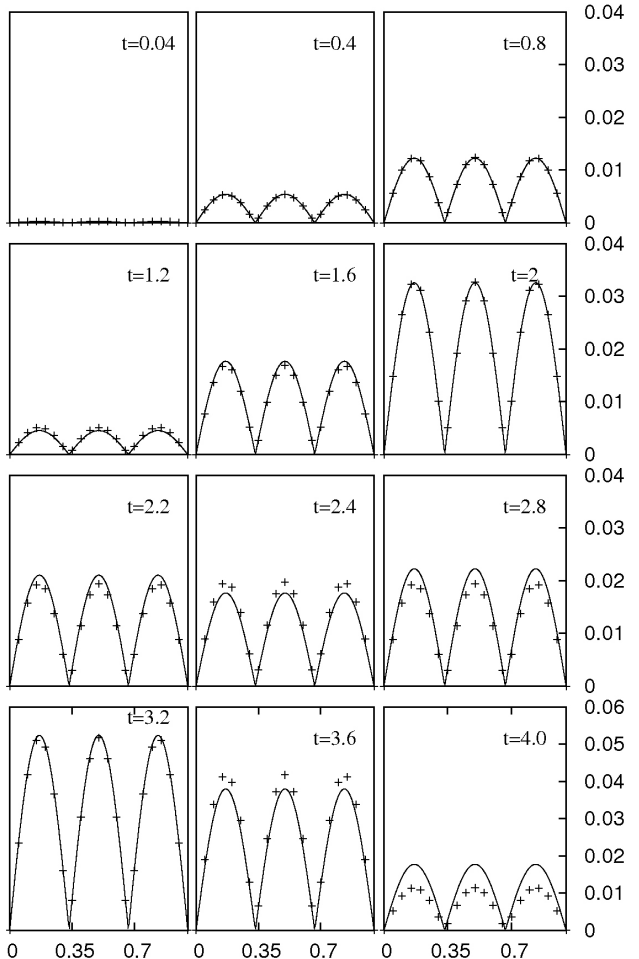


FIGURE 13. Comparison of the error at the axis $y = 0$ for the particle in a two-dimensional box at various times, with resolutions $\Delta x = \Delta y = 0.01$ and $\Delta x = \Delta y = 0.005$ (divided by four) with the factor $\Delta t/\Delta x^2 = 0.1$. When doubling the resolution, the error is four times smaller, indicating second-order convergence of the error to zero. The fact that the plots up to around $t \sim 2$ are still superposed indicates second-order convergence of the calculation up to this time; after this value of time, the solution is not second-order convergent anymore. However the convergence can be preserved for longer when the resolution is increased.

5.1.2. Numerical solution

This time, Schrödinger's equation for the particle in two dimensions and Cartesian coordinates reads

$$i \frac{\partial \Psi}{\partial t} = -\frac{1}{2} \left(\frac{\partial^2 \psi}{\partial x^2} + \frac{\partial^2}{\partial y^2} \right),$$

and its MoL discretized version reads:

$$\begin{aligned} \frac{\partial \Psi}{\partial t} &= \frac{i}{2} \left(\frac{\Psi_{j+1,k}^n - 2\Psi_{j,k}^n + \Psi_{j-1,k}^n}{(\Delta x)^2} \right. \\ &\quad \left. + \frac{\Psi_{j,k+1}^n - 2\Psi_{j,k}^n + \Psi_{j,k-1}^n}{(\Delta y)^2} \right) \\ &\quad + O(\Delta x^2, \Delta y^2). \end{aligned}$$

which we solve again using the third-order Runge-Kutta time integrator (5). We apply Dirichlet boundary conditions setting, the wave function to zero at the boundaries. In Fig. 12 we show the wave function obtained numerically at various times.

In Fig. 13 we show the comparison of the error when two resolutions are used. Second-order convergence to zero is found on a projection of the error along the $y = 0$ axis.

5.2. 2D harmonic oscillator

5.2.1. Exact solution

In this case, the potential is $V(x, y) = \frac{1}{2}K(x^2 + y^2)$. After applying separation of variables $\Psi = e^{-iEt}X(x)Y(y)$, the solution for the spatial part of the wave function is:

$$\begin{aligned} X_{n_x}(\xi) &= \sqrt{\frac{1}{\sqrt{\pi}2^{n_x}n_x!}}e^{-\xi^2/2}H_{n_x}(\xi) \\ Y_{n_y}(\eta) &= \sqrt{\frac{1}{\sqrt{\pi}2^{n_y}n_y!}}e^{-\eta^2/2}H_{n_y}(\eta), \end{aligned} \quad (22)$$

where $\xi = \sqrt{\alpha}y$ and $\eta = \sqrt{\alpha}x$, and with the permitted energy values

$$E_{n_x, n_y} = n_x + n_y + 1.$$

Then the complete full time-dependent solution and its real part are:

$$\begin{aligned} \Psi(x, y, t) &= \sqrt{\frac{1}{\pi 2^{n_x}n_x!2^{n_y}n_y!}} \cdot \\ &\times e^{-iE_{n_x, n_y}t}e^{-\frac{x^2}{2}}e^{-\frac{y^2}{2}}H_{n_x}(x)H_{n_y}(y) \\ \Re(\Psi(x, y, t)) &= \sqrt{\frac{1}{\pi 2^{n_x}n_x!2^{n_y}n_y!}}e^{-\frac{x^2}{2}}e^{-\frac{y^2}{2}} \cdot \\ &\times H_{n_x}(x)H_{n_y}(y)\cos((n_x + n_y + 1)t). \end{aligned}$$

As before, we choose this exact solution at $t = 0$ to be our initial data to be evolved using the Schrödinger equation and we do not plot the exact solution anymore and proceed to show the numerical results.

5.2.2. Numerical solution

In Fig. 14 we show the real part of the wave function and the density of probability at various times. The case corresponds to $n_x = 3$ and $n_y = 2$. Once again, as expected, our code shows an oscillating wave function and a frozen density of probability.

The domain has boundaries far from the region where the dynamics is going on, that is, the evolution of the wave function is localized as in the one-dimensional case, thus applying Dirichlet boundary conditions, setting the wave function to zero at the boundaries, suffices.

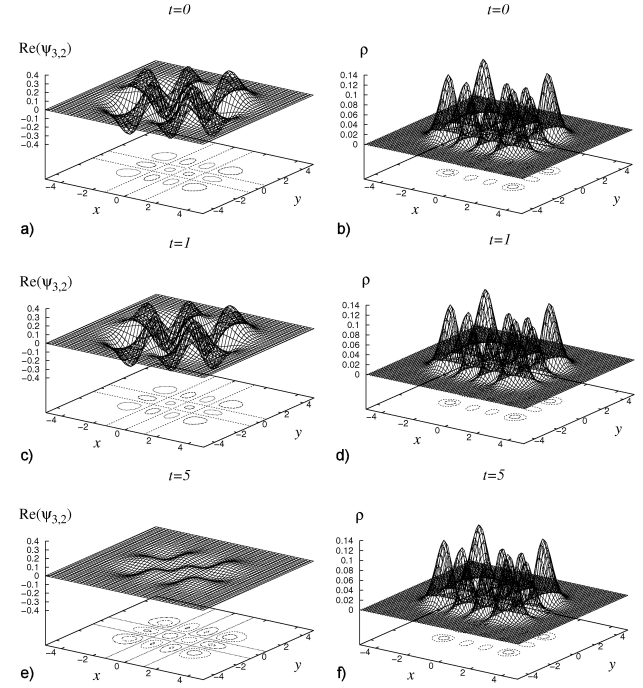


FIGURE 14. Numerical solution of a particle in a two-dimensional harmonic oscillator potential. We show the real part of the wave function and the density of probability for the case $n_x = 3$ and $n_y = 2$. The resolution used is $\Delta x = \Delta y = 0.1$ with the factor $\Delta t/\Delta x^2 = 0.1$. The domain used for the calculation is $x \in [-7, 7]$ and $y \in [-7, 7]$.

5.3. Example in 2D

When dealing with systems that allow the wave function out of the domain or does not guarantee that the wave function is localized in a finite domain, it is important to deal with boundary conditions on the wave function that distinguish between outgoing and incoming modes. However, in order to provide more usual, simpler boundary conditions on the wave function we introduce the concept of sponge, that is, we define a region of the spatial domain that acts as a sink of particles. This technique has been applied in various studies involving the solution to Schrödinger's equation, for example self-gravitating Bose condensates [11] and stabilization of an atomic gas [12]. The idea is to prevent the density of probability from being reflected back from the boundaries which eventually would pollute the calculations.

The sponge-sink region is defined on a chunk of the domain near the numerical boundary. This sponge is produced by assuming that in this region the system has an imaginary potential. In order to understand what the effects are on the wave function of the addition of an imaginary potential, we consider the Schrödinger equation

$$i\frac{\partial\Psi}{\partial t} = -\frac{1}{2}\nabla^2\Psi + V\Psi,$$

where V is a general potential. We also write the complex

conjugate of this equation:

$$-i \frac{\partial \Psi^*}{\partial t} = -\frac{1}{2} \nabla^2 \Psi^* + V^* \Psi^*,$$

where we have assumed that the potential has a non-zero imaginary part. As usual, one multiplies the first equation times Ψ^* and the second by Ψ , then adds both results and one obtains the continuity equation for the density of probability:

$$\begin{aligned} \frac{\partial(\Psi\Psi^*)}{\partial t} + \nabla \cdot \left[\frac{i}{2} (\Psi\nabla\Psi^* - \Psi^*\nabla\Psi) \right] \\ = 2\Psi\Psi^* \text{Im}(V). \end{aligned} \quad (23)$$

When V is real, there is conservation of the density of probability. Otherwise, the system has a sink or a source of particles, depending on the sign of $\text{Im}(V)$. The remaining problem is the choice of the $\text{Im}(V)$ profile that goes to zero in the region containing the physical system, and to a negative number when approaching the sponge-sink region near the numerical boundaries. The profile we choose is as follows:

$$\text{Im}(V) = -\frac{1}{2} V_0 \{2 + \tanh[(r - r_c)/\delta] - \tanh(r_c/\delta)\},$$

which is a smooth version of a step function [11]. In this expression, V_0 is the depth of the imaginary potential well, r is the radial coordinate ($r = x$ in the one-dimensional case and $r = \sqrt{x^2 + y^2}$ in the 2D case); r_c is the radius at which the step is centered, δ is the width of a transition region. In Fig. 15 we show the sponge potential used in the example below.

In Refs. 11 the transmission and reflection coefficients are calculated for a step function potential, and the maximum absorption corresponds to the case of a large region for the sponge and a small V_0 . In practice such conditions cannot be afforded, and then the smoothed version of the step function helps to clean up the modes that otherwise would be reflected back into the physical domain. The conditions at the boundary can be those of the faces of a box used earlier, and then the reflected modes are absorbed in the sponge region.

Using this technique, we proceed to show our last example: the stabilization of a soft-core model of an atomic gas. In this case we study the response of a distribution of atoms to the interaction with a laser-like potential. We restrict this to the case in which the system has s-lab symmetry, that is, what happens at the plane $z = z_0$ happens also for any other $z = \text{constant}$ plane. The Schrödinger equation is used to model the behavior of the gas [12], so that the wave function represents the dynamics of the gas. Thus the two-dimensional examples above contain the necessary technology for simulating this case.

One considers that the gas is made of hydrogen-like atoms. The model for the potential over the electron of each atom is Coulombian, that is, $1/\sqrt{x^2 + y^2}$; however, we apply Rydberg's soft core model [13], in which case the atom potential is $1/\sqrt{\alpha^2 + x^2 + y^2}$, where α plays the role of the smoothness parameter and avoids the singularity at the origin. The interaction with the laser is approximated by the

dipole interaction with classical radiation [14]. Finally, the total potential to which the system is subject is

$$V = -\frac{Z}{\sqrt{\alpha^2 + x^2 + y^2}} + g(t)F[x \sin(\omega t) + y \cos(\omega t)],$$

where we have used $Z = 1$, and where we use units such that $\hbar = e = m = 1$, where e is the charge of the electron. Here ω is the frequency of the laser, $g(t)$ is a function that goes from zero to one in a finite time, and F is the laser intensity. Under the symmetry used, Schrödinger's equation driving the system reads

$$i \frac{\partial \Psi}{\partial t} = -\frac{1}{2} \left(\frac{\partial^2}{\partial x^2} + \frac{\partial^2}{\partial y^2} \right) \Psi + V\Psi.$$

We now carry out various simulations with different values of F in order to determine the effect of this parameter on the lifetime of the gas. In Fig. 16 we show the integral of the density of probability for various values of the laser intensity. These simulations were carried out for an initial wave function profile $\Psi(x, y, 0) = e^{-(x^2+y^2)}$, on the domain $x \in [-20, 20]$, $y \in [-20, 20]$, with spatial resolution

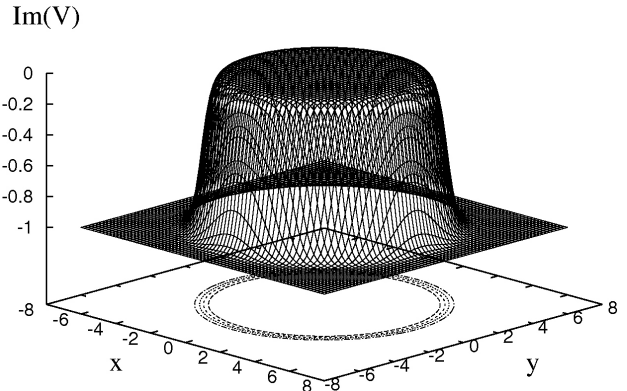


FIGURE 15. We show $\text{Im}(V)$ for the 2D domain with $V_0 = 1$.

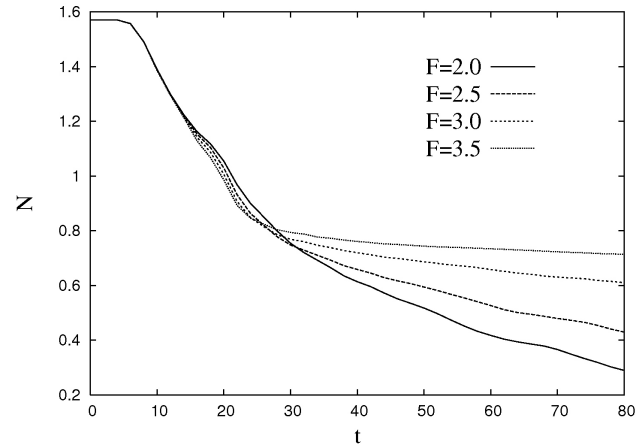


FIGURE 16. We show the decay of $N = \int \int \rho dx dy$ for various values of F .

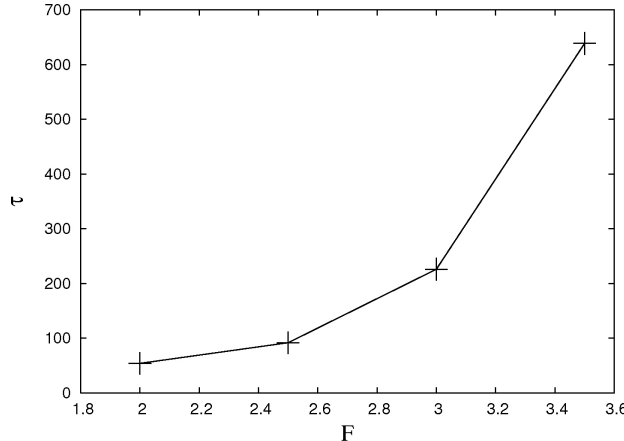


FIGURE 17. We show the lifetime (as defined in the text) for various values of F .

$\Delta x = \Delta y = 0.2$ and time resolution $\Delta t/\Delta x^2 = 0.1$. The sponge contains 25 points from the faces of the domain. The frequency of the laser was assumed to be $\omega = 1.2$, the smoothness parameter of the atomic model $\alpha = 0.8$. The intensity factor $g(t)$ used was a linear growing function from $t = 0$ to $t = 20$.

In order to estimate the lifetime of the gas, we produce an exponential fitting of the curves in Fig. 16 from $t = 30$ on, that is, we use the function

$$N = N_0 e^{-t/\tau},$$

where t is the time and τ is a naive but commonly used estimate of the lifetime of the system, N and N_0 are numbers proportional to the number of particles that have not left the numerical domain, and are freely chosen from the initial data, in our case an initial Gaussian wave function with amplitude and width equal to one (see above). In this case,

$$N = \int_{-20}^{20} \int_{-20}^{20} \rho dx dy$$

indicates the integrated density of probability that remains in the domain. The results of the fitting are shown in Fig. 17.

We have shown with this test problem that the intensity of the laser has an impact on the lifetime of the gas. The results shown here are pretty much consistent with those found in Ref. 12. This example could be extended for instance to discover the effects of changing the frequency of the laser ω on the lifetime of the gas.

6. Final comments

In this paper we have presented the finite difference approximation and applied it in finding numerical solutions to the

time-dependent Schrödinger equation in one and two dimensions. As examples we have presented the solution for the particle in a box and in a harmonic oscillator potential. These examples help in understanding:

- i) the evolution algorithm,
- ii) the time-dependent solution in terms of the wave function and the density of probability,
- iii) the checks of a unitary evolution,
- iv) the concept of convergence of the solution in the continuum limit.

As a non-standard problem, we also showed the evolution of solitonic solutions in one dimension. We expect this example to illustrate:

- i) what a solitonic solution is,
- ii) how periodic boundary conditions work.

In two dimensions we solved Schrödinger's equation that models a soft-core gas under a Laser-like potential. We expect the solution of this problem to illustrate:

- i) how a sponge works, and
- ii) how to deal with a time-dependent potential.

These tools could immediately be applied for instance:

- a) to the propagation of Bose condensates in optical lattices through the simple introduction of a spatially periodic potential, as in Ref. 15,
- b) the evolution of collapsing and exploding Bose condensates in different trap symmetries as in Ref. 16, and
- c) a garden variety of models based on the solution of the time-dependent Schrödinger equation related to condensates and solitons.

The code is also available in Ref. 17.

Acknowledgments

This work is partly supported by projects CIC-UMSNH: 4.9 and 4.11, PROMEP: UMICH-PTC-121 and UMSNH-CA-22.

1. L.P. Pitaevskii, *Zh. Eksp. Teor. Fiz.* **34** (1958) 1240; E.P. Gross, *J. Math. Phys.* **4** (1963) 195.
2. R. Becerril, F.S. Guzmán, and S. Valdez-Alvarado, in preparation.
3. J.W. Thomas, *Numerical Partial Differential Equations: Finite Difference Methods* (Texts in Applied Mathematics 22, Springer 1995).
4. S. López-Aguayo *et al.*, *Rev. Mex. Fís.* **52** (2006) 28.
5. B. Gustafsson, H-O. Kreiss, and J. Oliger, *Time Dependent Problems and Difference Methods* (Wiley-Interscience, 1996).
6. R.J. LeVeque, in *Numerical methods for conservation laws* (Birkhauser, Basel, 1992).
7. W.H. Press, S.A. Teukolsky, W.T. Wetterling, and B.P. Flannery, *Numerical Recipes in Fortran* (Cambridge University Press, 1992).
8. F.S. Guzmán, *Rev. Mex. Fís.* **53** (4) (2007) 78.
9. C. Sulem and P-L. Sulem, *The Nonlinear Schrödinger Equation* (Applied Mathematical Sciences v 139, Springer Verlag 1999).
10. R. Rajaraman, in *Solitons and Instantons* (North-Holland Personal Library, 1996).
11. F.S. Guzmán and L.A. Ureña-López, *Phys. Rev. D* **69** (2004) 124033.
12. D-I. Choi and W. Chism, *Phys. Rev. A* **66** (2002) 025401.
13. A. Patel *et al.*, *Phys. Rev. A* (1998) R2652.
14. K.C. Kulander *et al.*, *Phys. Rev. Lett.* **66** (1991) 2601.
15. D-I. Choi and Qian Niu, *Phys. Rev. Lett.* **82** (1999) 2022.
16. S.K. Adhikari, *Phys. Rev. D* **71** (2005) 053603.
17. <http://www.ifm.umich.mx/guzman/FreeCode/codes.html>